



Table S1. List of bacteria commonly found in the human gut microbiome. This list is derived from Shanmugham and Pan [59], detailing various microorganisms and their respective strains.

#	Microorganism	Strain
1	<i>Actinomyces odontolyticus</i>	ATCC 17982
2	<i>Akkermansia muciniphila</i>	ATCC BAA-835
3	<i>Alistipes putredinis</i>	DSM 17216
4	<i>Anaerofustis stercorihominis</i>	DSM 17244
5	<i>Anaerostipes caccae</i>	DSM 14662
6	<i>Anaerotruncus colihominis</i>	DSM 17241
7	<i>Pseudoflavonifractor capillosus</i>	ATCC 29799
8	<i>Bacteroides cellulosilyticus</i>	DSM 14838
9	<i>Bacteroides coprocola</i>	DSM 17136
10	<i>Bacteroides dorei</i>	DSM 17855
11	<i>Bacteroides eggerthii</i>	DSM 20697
12	<i>Bacteroides finegoldii</i>	DSM 17565
13	<i>Bacteroides intestinalis</i>	DSM 17393
14	<i>Bacteroides ovatus</i>	ATCC 8483
15	<i>Bacteroides pectinophilus</i>	ATCC 43243
16	<i>Bacteroides plebeius</i>	DSM 17135
17	<i>Bacteroides stercoris</i>	ATCC 43183
18	<i>Bacteroides uniformis</i>	ATCC 8492
19	<i>Bifidobacterium adolescentis</i>	ATCC 15703
20	<i>Bifidobacterium adolescentis</i>	L2-32
21	<i>Bifidobacterium angulatum</i>	DSM 20098
22	<i>Bifidobacterium bifidum</i>	DSM 20456
23	<i>Bifidobacterium breve</i>	DSM 20213
24	<i>Bifidobacterium dentium</i>	ATCC 27678
25	<i>Bifidobacterium longum</i>	DJO10A
26	<i>Bifidobacterium longum</i>	NCC2705
27	<i>Bifidobacterium longum subsp infantis</i>	str ATCC 15697
28	<i>Borrelia burgdorferi</i>	CA-11.2A
29	<i>Butyrivibrio crossotus</i>	DSM 2876
30	<i>Catenibacterium mitsuokai</i>	DSM 15897
31	<i>Clostridium asparagiforme</i>	DSM 15981
32	<i>Clostridium bartlettii</i>	DSM 16795
33	<i>Clostridium bolteae</i>	ATCC BAA-613
34	<i>Clostridium hiranonis</i>	DSM 13275
35	<i>Clostridium leptum</i>	DSM 753
36	<i>Clostridium methylpentosum</i>	DSM 5476
37	<i>Clostridium nexile</i>	DSM 1787
38	<i>Clostridium ramosum</i>	DSM 1402
39	<i>Clostridium scindens</i>	ATCC 35704
40	<i>Clostridium</i>	sp L2-50
41	<i>Clostridium</i>	sp M62/1
42	<i>Clostridium</i>	sp SS2/1
43	<i>Clostridium spiroforme</i>	DSM 1552
44	<i>Clostridium sporogenes</i>	ATCC 15579
45	<i>Clostridium symbiosum</i>	ATCC 14940
46	<i>Collinsella aerofaciens</i>	ATCC 25986
47	<i>Collinsella intestinalis</i>	DSM 13280
48	<i>Collinsella stercoris</i>	DSM 13279
49	<i>Coprococcus comes</i>	ATCC 27758
50	<i>Coprococcus eutactus</i>	ATCC 27759
51	<i>Dorea formicigenerans</i>	ATCC 27755
52	<i>Dorea longicatena</i>	DSM 13814
53	<i>Eggerthella lenta</i>	DSM 2243
54	<i>Enterobacter cancerogenus</i>	ATCC 35316
55	<i>Eubacterium dolichum</i>	DSM 3991
56	<i>Eubacterium hallii</i>	DSM 3353

57	Eubacterium siraeum	DSM 15702
58	Eubacterium ventriosum	ATCC 27560
59	Faecalibacterium prausnitzii	A2-165
60	Faecalibacterium prausnitzii	M21/2
61	Lactobacillus salivarius	UCC118
62	Methanobrevibacter smithii	ATCC 35061
63	Methanobrevibacter smithii	DSM 11975
64	Methanobrevibacter smithii	DSM 2374
65	Methanobrevibacter smithii	DSM 2375
66	Mitsuokella multacida	DSM 20544
67	Parabacteroides johnsonii	-
68	Parabacteroides merdae	ATCC 43184
69	Parvimonas micra	ATCC 33270
60	Photorhabdus luminescens	subsp laumondii TTO1
61	Prevotella copri	DSM 18205
62	Providencia alcalifaciens	DSM 30120
63	Providencia rettgeri	DSM 1131
64	Providencia rustigianii	DSM 4541
65	Roseburia faecis	M72/1
66	Roseburia intestinalis	L1-82
67	Ruminococcus gnavus	ATCC 29149
68	Ruminococcus lactaris	ATCC 29176
69	Ruminococcus obeum	ATCC 29174
70	Ruminococcus torques	ATCC 27756
71	Streptococcus infantarius subsp infantarius	ATCC BAA-102
72	Subdoligranulum variabile	DSM 15176
73	Victivallis vadensis	ATCC BAA-548

3

4

5

6

7

8

9

10

11

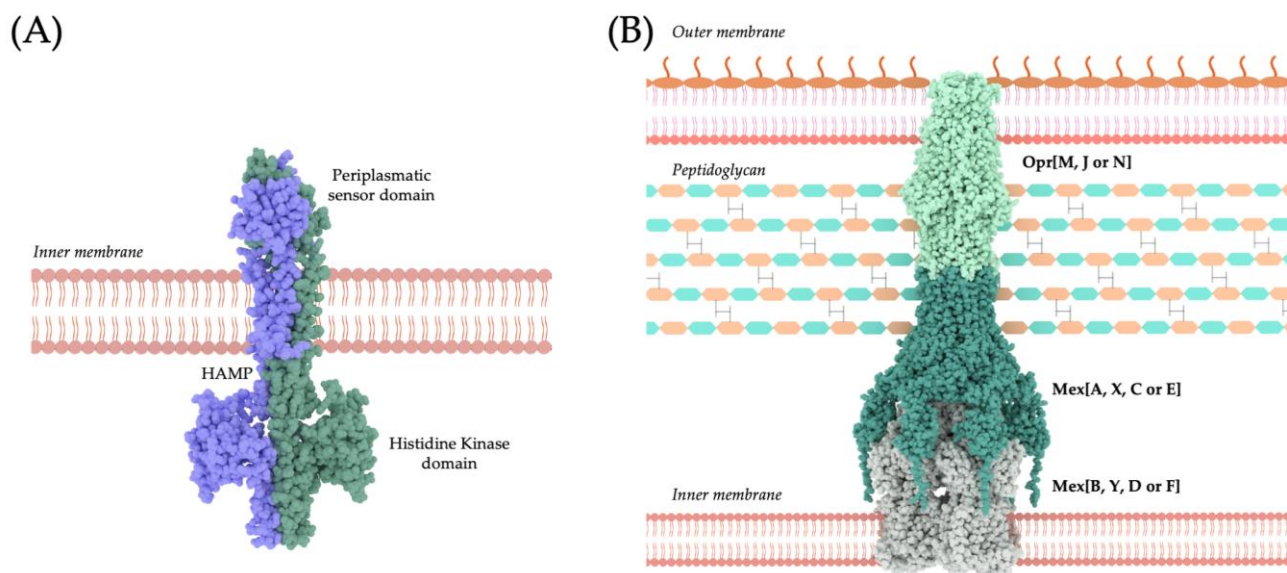


Figure S1. Types of essential proteins selected in the subtractive proteomics stage. This figure presents the three-dimensional structures of essential proteins that met all criteria used in the subtractive proteomics pipeline. A) Histidine Kinase, embedded in the inner membrane. B) A tripartite RND efflux pump, shown with its components spanning the inner membrane, peptidoglycan layer, and outer membrane.

13

14

15

16

17

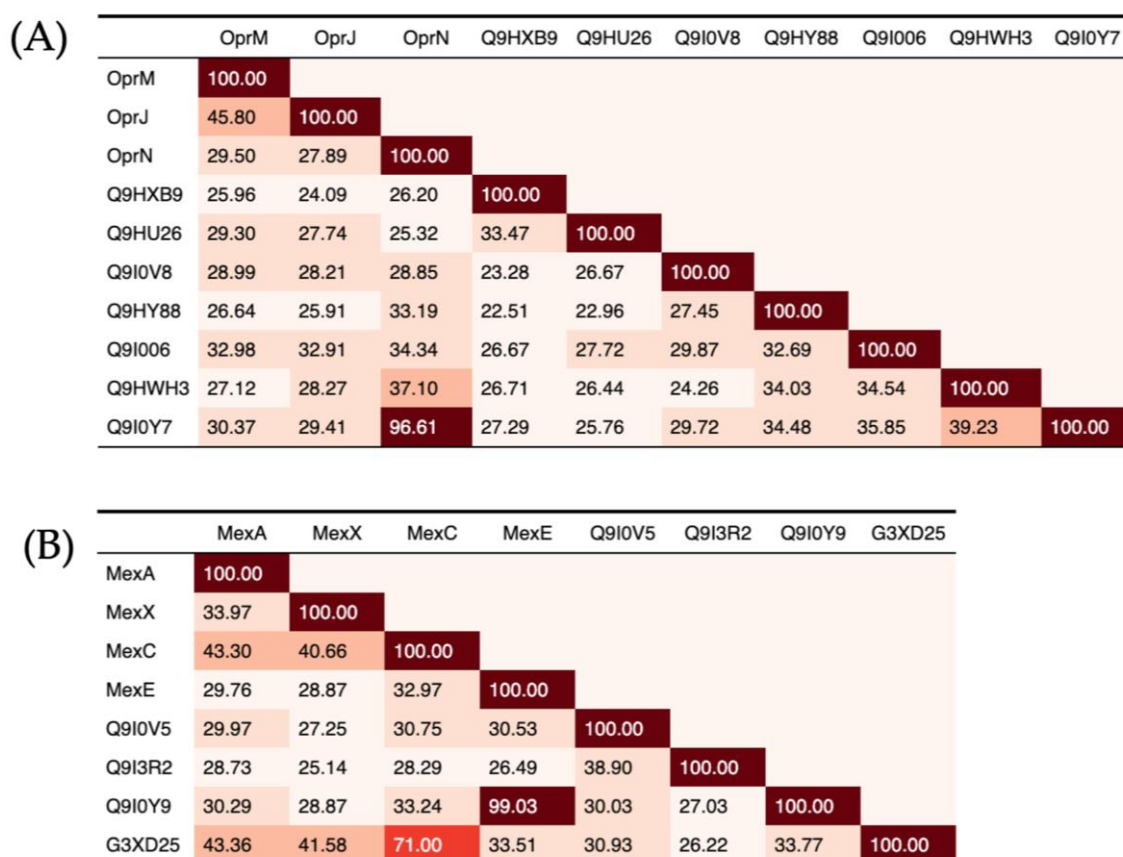


Figure S2. Sequence identity heatmap of the studied proteins. A) OMF-type proteins studied and the canonical OprM, OprJ and OprN proteins. B) MFP-type proteins studied and the canonical MexA, MexX, MexC and MexE proteins. The darker the color, the higher the sequence identity of the compared protein pair.

Table S2. Selected RND proteins from the complete protocol for drug repurposing. RND proteins, detailing their UniProt ID, the closest matching structure available in the Protein Data Bank (PDB), the percentage of sequence identity against the PDB protein, and their amino acid sequences for both OMF and MFP proteins.

Protein Type	Uniprot protein accession ID	PDB ID of most related protein	% sequence identity of the closest protein	Aminoacid sequence
Outer Membrane Factor	Q9I0Y7	5AZP	100%	MIHAQSIRSGLASALGLFSLALLSACTVGPDPYRTPDTAAAKIDAT ASKPYDRSRFESLWWKQFDDPTLNQLVEQSLSGNRDLRVAFARL RAARALRDDVANDRFVVTSRASADIGKGQQPGVTEDRVNSER YDLGLDSAWELDLFGRIRRLQLESSDALSEAAEADLQQLQVSLIAE LVDAYGQLRGAQLREKIALSNLENQKESRQLTEQLRDAGVGAEL DVLRADARLAATAASVPQLQAEARARHRIATLLGQRPEELTV LSPRDLPAITKALPIGDPGELLRRRPDIRAAERRLAASADVGVAT ADLFPRVSLSGFLGFTACRGSGQIGSSAARAWSVGPSISWAAFDLG SVRARLRGAKADADAALASYEQVLLALEESANAFSDYGKRQE RLVSLVRQSEASRAAAQQAIRYREGTTDFLVLLDAEREQLSAED AQAQAEVELYRGIVAIYRSLGGGWQPSA

	Q9HXB9	1YC9	36.73%	MVGSFVGFLLVVFSAISGCVSTGDIAPAAATLDANALATDHAIIQA AAREAGWPQAQWVKVYADPQLDAWIEKALDGNPGLAVAHA RVRQAKSMAGLVESIESPQIEGKGS�VRHRWPDDYFYGPGDLAR TTSWNNSTEIGLNYKLDLWGRDRSDSERAVDLAHMAAAAEARQ AQLEGENIVRAYVQSLQYAEMDIKAMLQQQRDILALAQRR LRGGIGTHFEVSQAIEVPLPETERRIEVIDEIIQLTRNLLAALAGKG PGEGRITRRPSLNLAQAQPSLPSALPAELLGRRPDVVARWQVAA LAKGVDVARADFYPNVDLMASVGFSAVGGGMLEFFRSKYTYTS AGPAVTLPIFDGGRRLRSQLEAAAGYDAVEQYNQTLVDALKN ISDQLIRLHSDIQKDFAAQSVASAKQTYDIATLAYQRGRLTDYLN VLNAQTRLFQQQLVQEQQVQAARLAHAHSLLTALGGGVGAGAD TPAQRKLAPENVPVRAVSSR
	Q9I0V8	1WP1	28.87%	MKHTPSLLALALVAALGCAIGPDYQRPDLAVPAEFKEAEGWR RAEPRDVFQRGAWWELYGDQTLNDLQMHLSRNQTLAQSVAQ FRQAEALVRGARAAFFPSITGNVGKTRSGQGGGDSTVLLPGGST VSSGGSGAISTSYSTNLSVSWVEVDLWGLKRRQLEANQASLHASA ADLAAVRLSQQSQAQNYLQLRVMDEQIRLLNDTVTAYERSLK VAENKYRAGIVTRADVARTQLKSTQAQAIKLYQRAQLEHA IAVLVGLPPAQFNLPVAVSPKLPDLPAVVPQLLERRPDIASAER KVISANAQIGVAKAAYFPDLTSAAGGYRSGSLSNWISTPNRFWS IGPQFAMTLFDGGLIGSQVDQAEATYDQTVATYRQTVLDGFREV EDYLVQLSVLDEESGVQREALSAREALRLAENQYKAGTVDYTD VVTNQATALSNERTVLTLGSRLTASVQLIAMGGGWDSADIER TDERLGRVEEGLPPSP
	Q9I006	5IUY	36.44%	MKGTPLLLIASLALGACSLGPDFTFRPDRPAPGEWSLQAAAGNPS HLAAAPLAAQWWTLFDDAQLNALLQVRQANLDRSAAARL QQSRAIRRLSGGDALPSVDASGNYQRRTTSAGLFDPSGKAGKG NYNHALAGFDASWELDFWGRVRRLEAADATVEASENELRDV QVSVLAEAAARDYIQLRGEQNRAAIIIRDNLETARRSLELTRRLAN GVATDLEVAAQALAQVASMEARLPEVEKNQAHLVNALGLVGAS PGSLLAELGPARAIPRPPGSPVPGLPSELAQRRPDIRRAEARLHA ATASIGVAKADFYPRITLNGNFGFESLQLSSLGDWDHRQFAIGPA FSLPIFEGGRLRGRLELREAQQQEAIDYQRTVLRAQEVDDAMH DYAANQRRQERLGEAVAQNRRLQSAREQYRAGAVDFLSVLD SRQLLDNQEQQVASDEAVSLTLVNLKALGGGWSPTSDPASG
	Q9HU26	1YC9	36.90%	MPFPLLHPWPQRLALASAILLAAGCVTSEGLEPNARLQPAQALQ AGRSLDGVALSPPAAWPRQDWWTGLGDRQLDQLIGEALQGTDP LQIAEARARQAAATAQAQDAARQPTLDAKASYSGIRAPTSVAP APLGGRYSAIKYLSLGFNYDFDLWGGERAAWEAALGQANAARI DSQAARIGLSASIAARAYSDLAHAFTVRDLAEEELKR5QRMTLSQ KRMSAGLDSKVQLQQTQTQLATARQQLSAAEQDIASARIALAV LLGKGPDGRLELQRPQPLNPASLSLPVLPSELLGRRADIVAAAR WRVEAARRNIDSAKTEFYPNLNLGAMAGLAAHSTSDVLQAPSR FFQVAPAIPLPFDGGRRRANLAERDADYDLAVGQYNKTLVQAL GEVSDDLKGLRSLEQQVIDQRQARDIARNSFDLAMRRYGEGVGS YLDALSVQQQLLVAERQLASLESQQIDLVSQVLQALGGGFQPD RSAALATAKAPAE
	Q9HWH3	5IUY	39.86%	MKRSYPNLSRLALALAVGTGLAACSVGPDYQRPQSPPPRVASEH LGEFSGERREAPWWSFFDDPQLVRLVDQALARNHDIREARANL RSARALFDDRWDQLPQVTSQAGYSRSIEQQLDYDGEPRRLAE SYRAGFDAQWEIDLFGRLGRLSDAALARAEEAADLRLVRLSIA ADTARAYFEIQGYQRRLDVARAQVRSWRDTLELTRSSLQLGSL PEDVENAQANLLRSEAAIPPLTTALESARYRLDVRGEAPGSGAP ILDGGAAAPLAKNPLPGDVDRILQRPDVVSAERQLAATEDVGA AATAELYPRLDLGGFIGFFALRSGDLGSASRAFELAPSVSWPAFR LGNVRARLRAVEAQSDAALARYQRSLLAQEDVGNALNQLAE HQRRVLALFQSATHGANALEIANERYRAGAGSYLAVLENQAL YQIREELAQAETASFVNIALYKALGWGSGDLAPGAGQLAAGE TAGANR
	Q9HY88	5AZO	35.57%	MKPYLRSSLALILLGGCAAAGVGPDYAPPSASAPASFGAMPAGIDG SGVEIEWWRGFDEPALESILQRALAANLDIALAGARLDEAKALL RENREEFLPRGGPAFDYQARRRGEVETPAGQQORDIETYRGALDA SWEIDLFGVRVRSVEAAEAQAGSREALLRNVQASVAATVAMSW FQLQGIEAELAVVHDIAGNQQRDSLEMVERLSAGSAHEFDRLRA EALLHNVEAAVPLERRRAATRNALAVLLAEAPQAFSPVVARA SGERLTLRTLGVGDPAGLLARRADIAAERNLAAATARIGVETA GLYPQVEVRGSIGLVAGNLDALDESGTSFNVLPVIRWALLDRG RVWARIAASEARAQEAALILYDRTVLRALQETDDAFNGYGAAAD RLRLRLLEATANREAAARLARERFVQGDGEYLDVLEAERSDYLSR RALSIARTEQRLAVVGIYKALGGGWEACAGARRCGVATDDTSP GVARQRDSRS
Membrane Fussion Protein	Q9I0V5	5N5G	33.33%	MTPTTGKSKFRTLRLPWLTALFAAVIGLVMWLAAPASAPSSDG RPGRGKPGGAALPKANALTGVVARVEQGDALHFNALGTVTA FNTVNVKPRVNGELVKLVLFQEGQEVKAGDLLAVDPRTYKAAL AQAEGLTMQNQAQLKNAEIDLQRYKGLYAEDSIKQTLDTQEA QVRQLQGTIRTNQGVDDARLNLTFTEVRAPISGRLLGRQVDIG NLVTSGDTTPLVVITQVKPISVVFSLPQQQIGTVVEQMNGPGKLT VTALDRNQDKVLAEGTLTTLDNQIDTTTGTVKLKARFENADGK

				LFPNQFVNVRLLAQTLKGVLTIPANAVQRGTNGIYVYVVGADN KVSQRSVAIGTSENERVVVESGLKAGEQVVVEGTDRLRDGMVLR VAEASPOVLEGEPOKQPOTGRPSGLQGDSVSGSGSAE
Q9I0Y9	5V5S	34.53%		MEQSSHFSWRYPLALAAVLVLSACGKAPETTQGMAAPKVSVAE VIEQPLNEWDEFTGRLEAPESVELRPRVSGYIDRVAFHEGALVKK GDLLFQIDPRPFEEAEVKRLEAQLQQAARAAQARSVNEAQRGERLR ASNAISAEADARTTAAQEAKAAVAATQAQLDAARLNLSTFRIT APIDGRVSRAEVTAGNLVNSGETLLTTLVSTDKVYAYFDADERV FLKYVELARQAGRDTRSESPVYGLSSEEDGNPHLGRDLDFLDNQV NPRTGTIRGRAVFDNAKGEFTPLGYVRLKLVGSKTYAATLIKDEA VGTDLGKKFVLVDGDNKTVYRTVEMGPKLEGLRIVRSGLSKGD RIVVNGLQVRPQGMQVDPQKVMASADTLATLARLRQSVGDSE PPKVAASKDNATRNEPRG
Q9I3R2	5V5S	32.09%		MQALRSGGGRVLVGVLAAGLVAFGGWAWLGGDAGAKAAPAP ARVPVIVARVERRDVEQQV SGIGTVTSLHNVTQIDGQLTRLLVSEGMVEAGELLATIDDR AVVAALEQAQASRASNAQLKSAEQDLQRYRSLYAERAVSRQL LDQQQATVDQLRATLKANDATINAERVRLSYTRITSPVSGKVGIR NVDVGNLVRVGDSLGLFSVTQIAPISVVFSLQQEQLLQLQALLGG EAAVRAYSRDGGSALGEGRLLTIDNQIDSSTGTIRVRSFDRQA RLWPGQFVAVSLHTGVRRDQLVLSSKAVRRGLEGNFVYRVADD RVEAVPVRVLQDIDGLSVVEGLASGDQVVVDGHSRLMPGALVD IQEPRPSLAQATERRP
G3XD25	5V5S	46.82%		MADLRAIGRIGALAMAIALAGCGPAEERQEAEMVLPVEVLTV QAEPLALSSELPGRIEPVRVAEVRARVAGIVVRKRFEEGADVKG DLLFQIDPAPLKAASVRAEGELARNRAVLFEAQARVRRYEPLVKI QAVSQQDFDTATADLRSAEAAATRSQAADLETARLNLGYASVTA PISGRIGRALVTEGALVGQGEATLMARIQQLDPIYADFTQTAAEA LRLRDALKKGTAAAGDSQALTLRVEGTPYERQALQFADVAVD RGTGQIALRGKFANPDGVLLPGMYVVRVTPQGIDNQAILVPQR AVHRSSDGSAAQVMVVGADERAESRSVGTGMVQGSRWQITEGLE PGDRVIVGGLAAVQPGVKIVPKPDGAQAQAQSPAPQQ

30

31

32

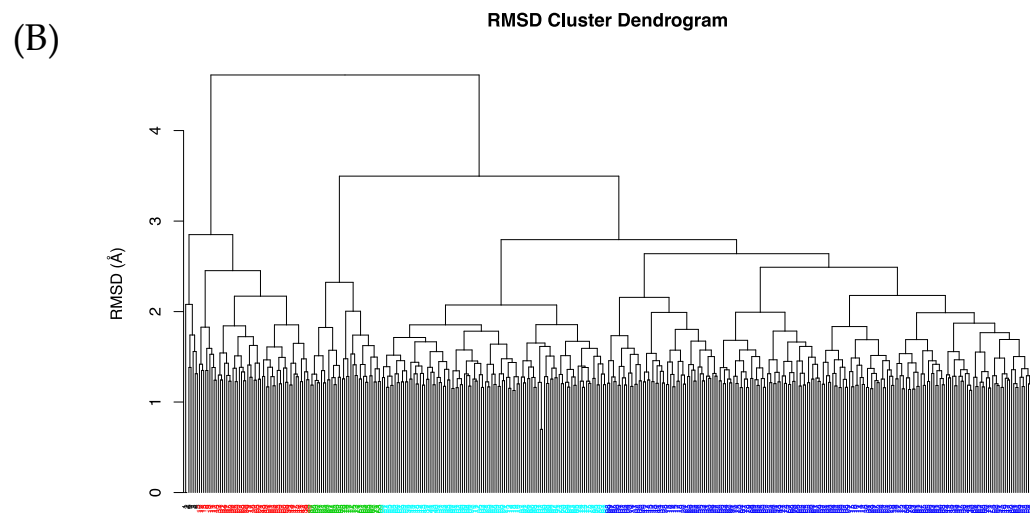
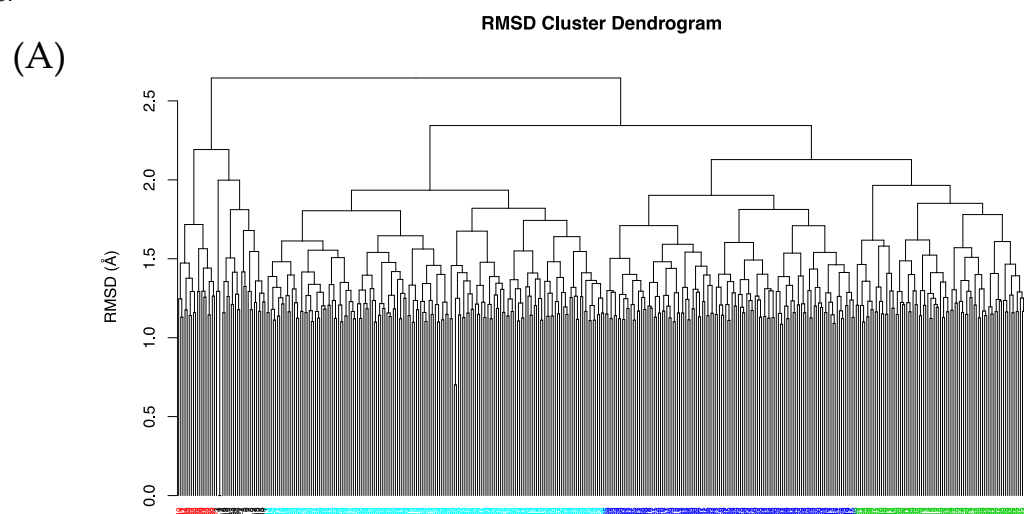
33

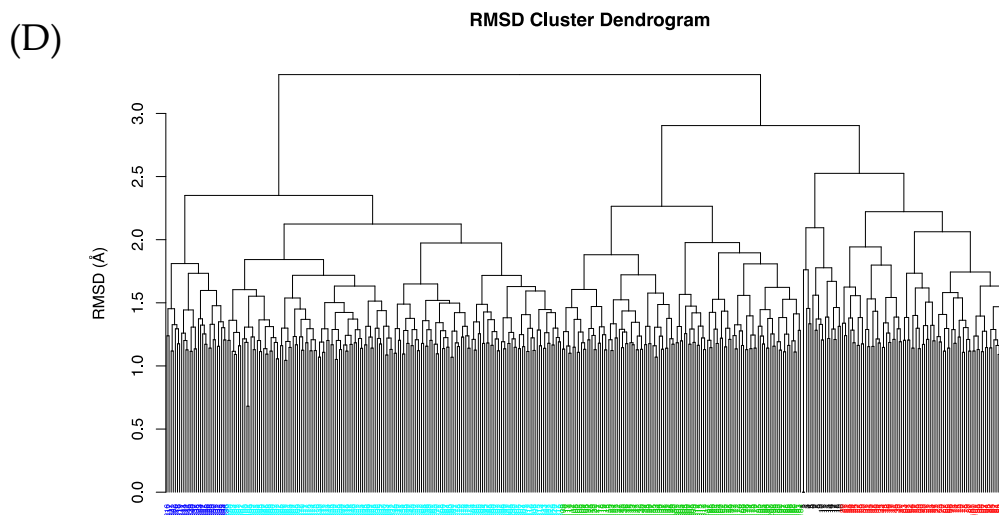
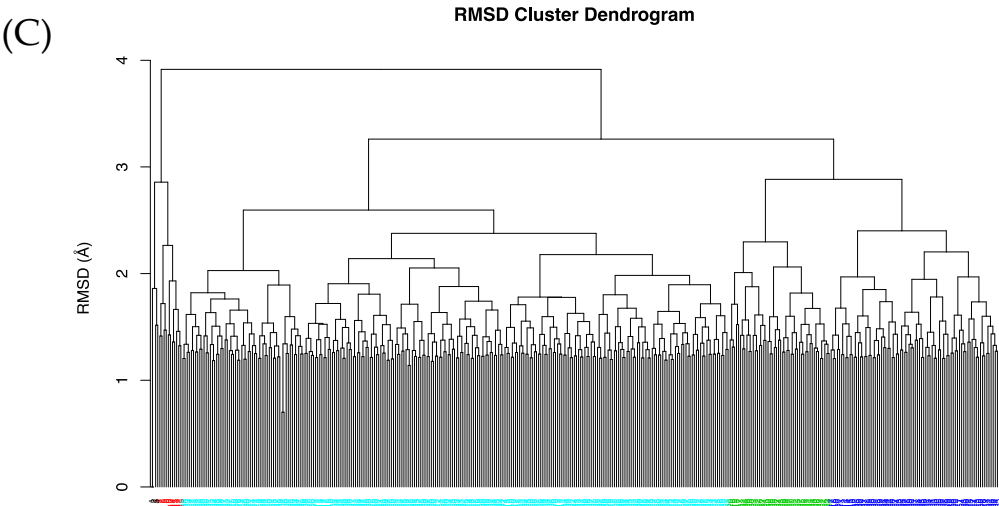
34

35

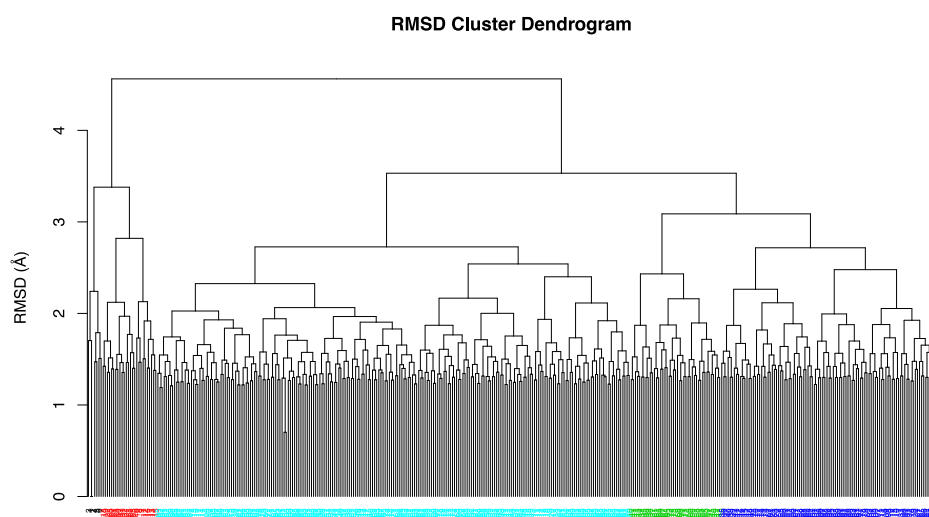
36

37

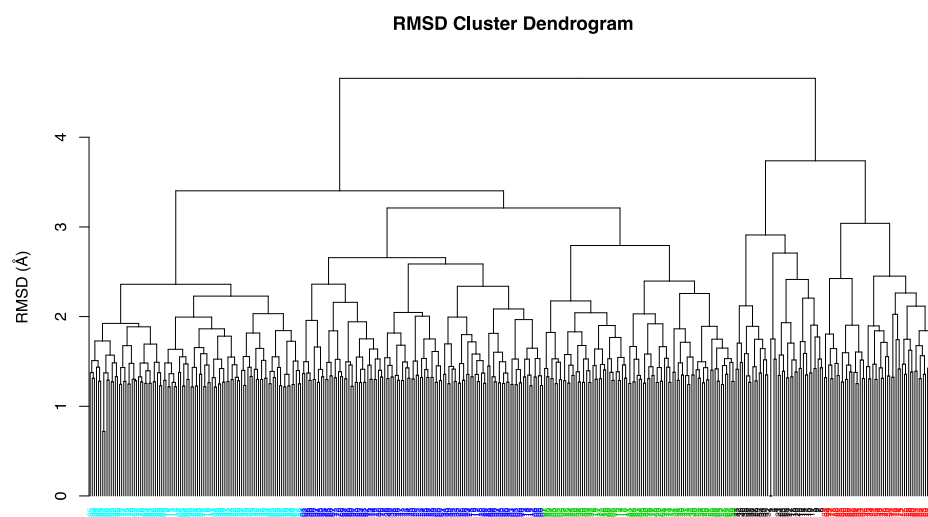


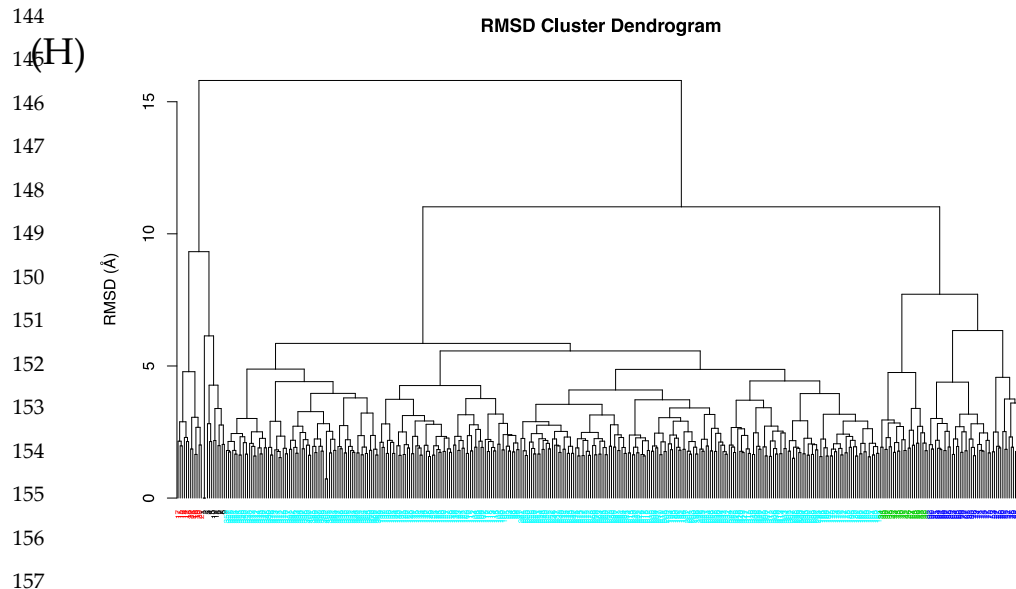


(E)



(F)





170
171
(I)

172

173

174

175

176

177

178

179

180

181

182

183

184

185

186
(J)

187

188

189

190

191

192

193

194

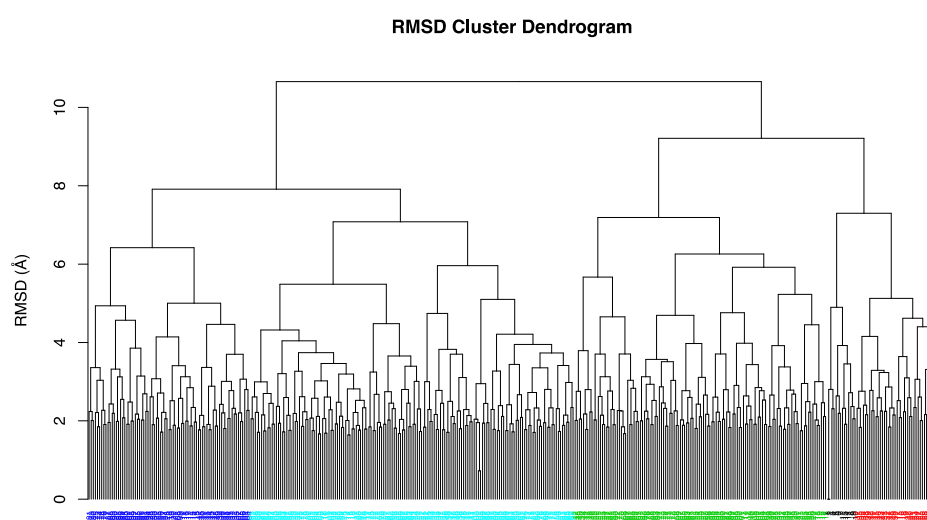
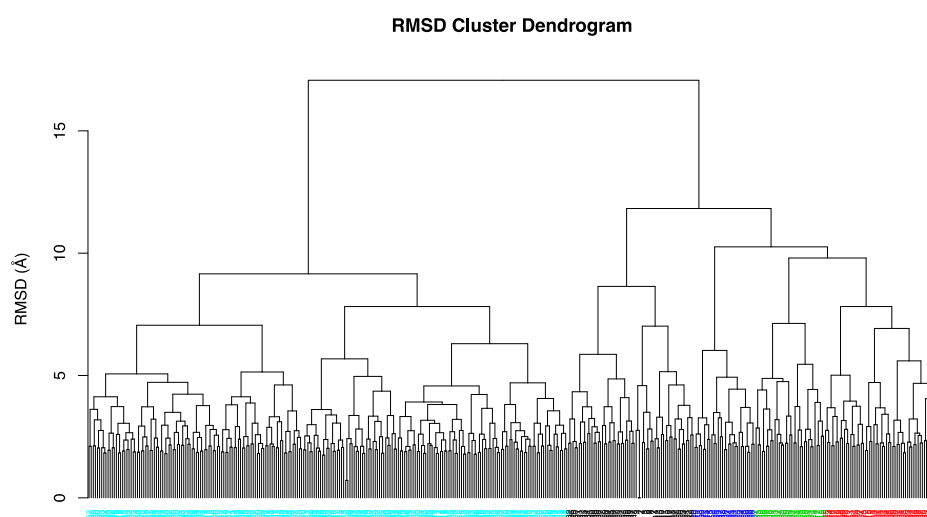
195

196

197

198

199



164

165

166

167

168

169

200

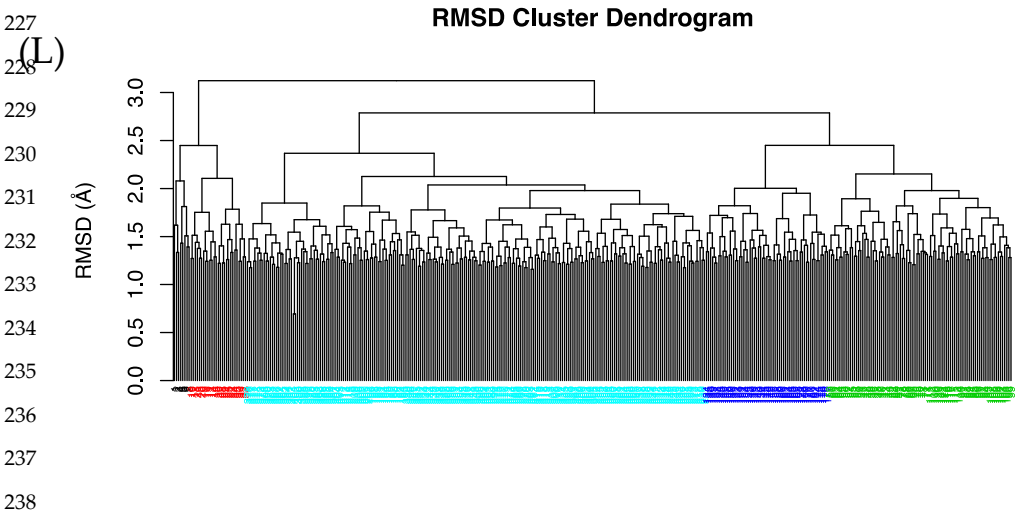
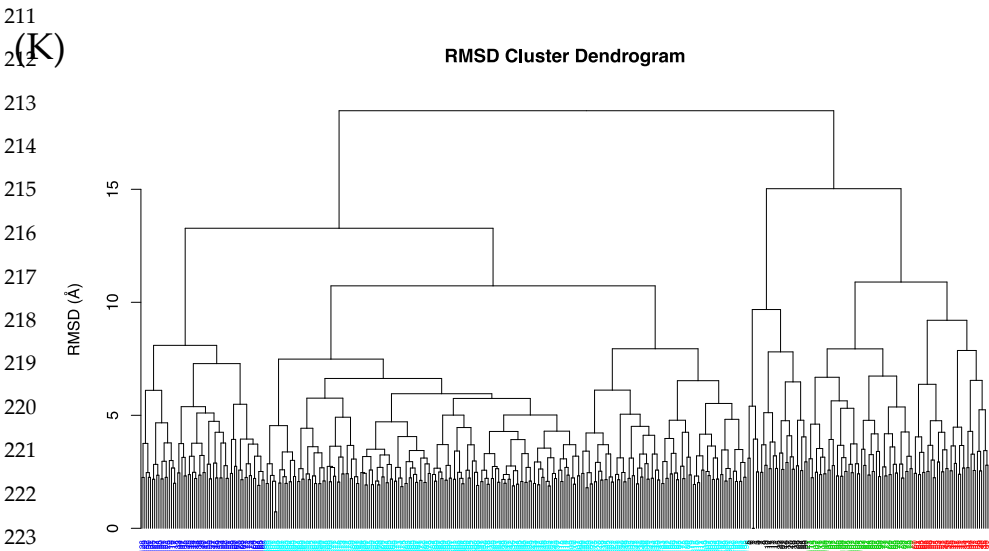
201

202

203

204

205



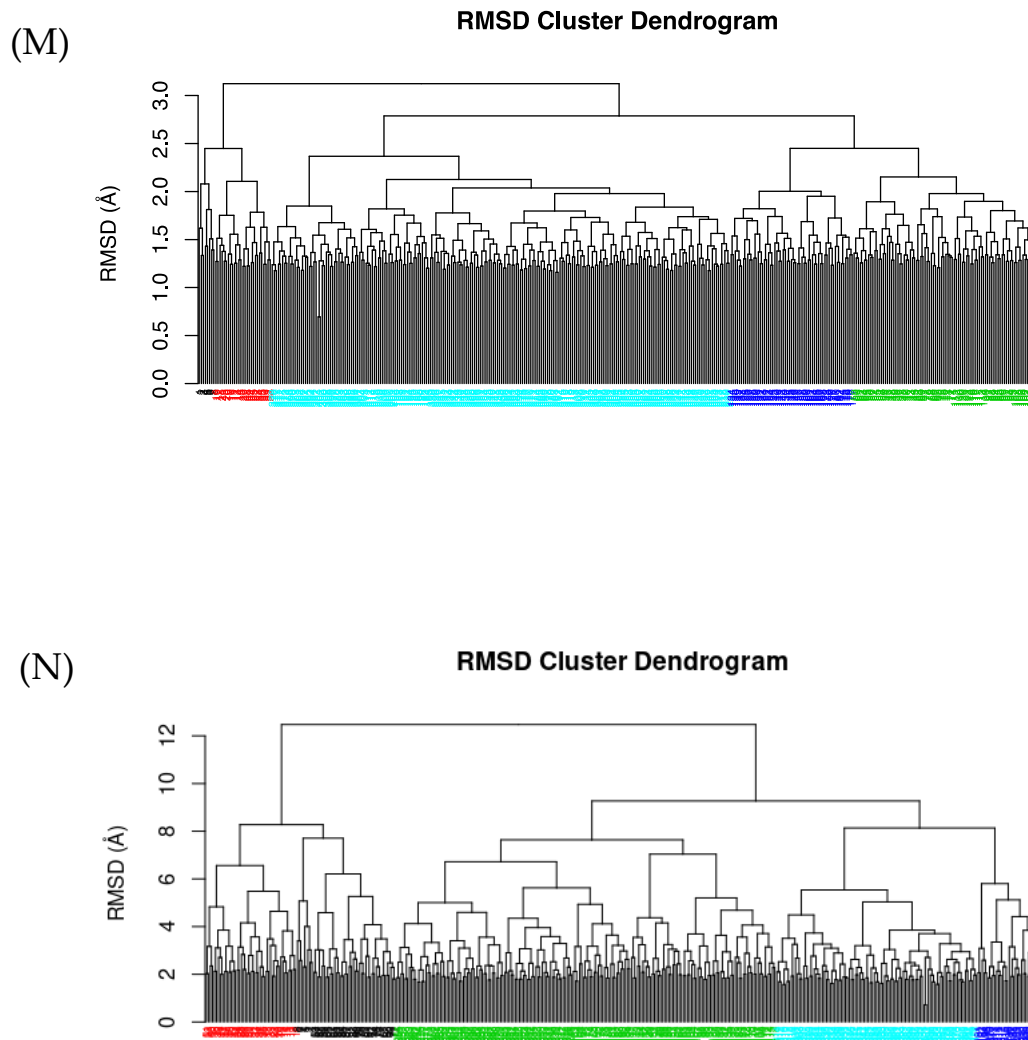


Figure S3. Cluster dendrogram calculated from the RMSD trajectories. Cluster dendrograms for OMF-type proteins, MFP-type proteins, and control proteins. Each color represents a cluster of frames from the MD trajectory with structural similarity. For OMF-type proteins: A) Q9I0Y7, B) Q9HXB9, C) Q9I0V8, D) Q9I006, E) Q9HU26, F) Q9HWH3, G) Q9HY88. For MFP-type proteins: H) Q9I0V5, I) Q9I0Y9, J) Q9I3R2, K) G3XD25. For control proteins L) OprM, M) MexA, N) MexB. The length of each cluster indicates the number of trajectory frames sharing structural similarity. While the image resolution may not allow for detailed viewing of cluster numbering, the relative size of each cluster reflects the population density of that conformation during the trajectory.

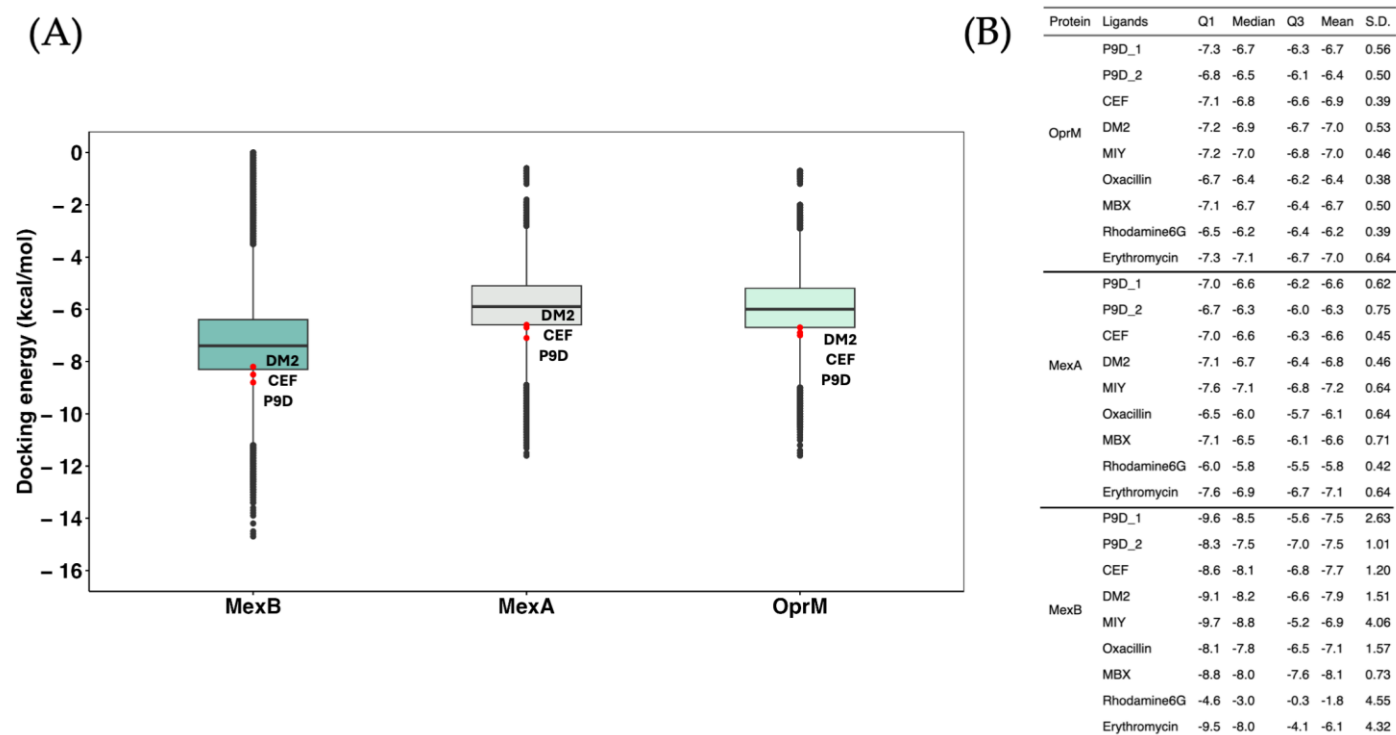


Figure S4. Docking binding energy of drug-repurposed and control compounds. A) The distribution of docking energy for the 5,712 repurposed drugs and 8 RND pump inhibitors used as controls across the proteins MexB, MexA and OprM. The boxplots illustrate the range of docking energies, with more negative values indicating stronger binding affinities B) Descriptive statistics of the 8 control inhibitors, including the first quartile (Q1), median, third quartile (Q3), mean, and standard deviation (S.D.) of the docking energies. Note that the P9D inhibitor has two tautomer forms (P9D_1 and P9D_2), which are represented separately.

Table S3: Descriptive statistic of promolecular energies for the 7 OMF proteins and 4 MFP proteins. This table provides the descriptive statistics of promolecular energies for the selected drug candidates (MK-3207, R-428, and Suramin) across the studied proteins. The statistics include the first quartile (Q1), median, third quartile (Q3), mean, and standard deviation (S.D.) of the promolecular energies.

Protein Type	Ligand	Q1	Median	Q3	Mean	S.D.
OMF	MK-3207	-0.136	-0.078	-0.026	-0.089	0.082
	R-428	-0.140	-0.080	-0.027	-0.093	0.089
	Suramin	-0.242	-0.169	-0.114	0.206	0.401

MFP	MK-3207	-0.132	-0.086	-0.044	-0.095	0.006
	R-428	-0.144	-0.89	-0.039	-0.099	0.075
	Suramin	-0.240	-0.162	-0.104	-0.177	0.103

308

309

310